Journal of ELECTRONIC MATERIALS, Vol. 49, No. 1, 2020
https://doi.org/10.1007/s11664-019-07481-3

The Variation of Microstructure and the Improvement of Shear Strength in SAC1205-xNi/OSP Cu Solder Joints Before and After Aging

COLLIN FLESHMAN[1] and JENQ-GONG DUH[1,2]

1.—Department of Materials Science and Engineering, National Tsing Hua University, Room 429, No. 101, Section 2, Kuang-Fu Road, Hsinchu 30013, Taiwan, ROC. 2.—e-mail: jgd@mx.nthu.edu.tw

The correlations between different Ni contents in Sn-1.2Ag-0.5Cu-xNi (wt.%; x = 0, 0.05, 0.1)/organic solderability preservative Cu solder joints and shear test performance before and after aging were probed. With the aid of electron back scattering diffraction analysis and a scanning electron microscope, complexity in microstructure of Ni-doped solder joints was investigated. The results of a slow speed shear test revealed that the peak force of solder joints was efficiently enhanced by the addition of Ni before and after aging. The improvement of mechanical strength was ascribed to the modification of microstructure by the introduction of minor Ni addition. Spread and tiny intermetallic compounds, and the oriented interlaced structure in Ni-doped solder joints acted as hindrances for propagation of cracks and dislocations. It is revealed that solder joints with minor Ni doping tend to exhibit better mechanical reliability in advanced electronic packaging no matter before or after aging.

Key words: Shear test, interlaced structure, microstructure, grain orientation, intermetallic compounds

INTRODUCTION

In electronics packaging, Sn-Ag-Cu (SAC) solders are widely used in this day and age to substitute traditional but toxic Sn-Pb solders, which have caused environmental and health issues.[1] Among the SAC family, low-Ag solders have been drawing industry's attention because of reduced costs of solders and superior properties such as drop performance, shock resistance, and so on.[2,3]

Besides reducing Ag content, minor doping is an effective method to fine tune the properties of lead-free solders.[4–6] Among additives, Ni is used most frequently in electronics industry on account of its remarkable performance in hindering the growth of intermetallic compounds (IMCs) and improving the mechanical properties of solders.[6,7] Apart from that, it is revealed Ni in solder joints could alter solidification microstructures.[6,8] The effect is even more apparent when it comes to smaller solder balls,[9] as the smaller ball size would affect undercooling of solders and thus influence the grain structure.[10]

For the structure of solder joints in a ball grid array (BGA), solder balls size is around 300–600 μm, yet the thickness of IMCs at the interface of solder and subsrate is only few microns at reflowed conditions.[11] Therefore, properties of solder balls play a key role in affecting the mechanical performance of whole solder joints. By altering the grain structure of β-tin and the precipitates in solders, mechanical strength of solder joints would be enhanced.

To focus on the effect of solder balls, a slow speed shear test was employed in this study. Chawla once proposed that higher strain rate would lead to IMCs-dominated fracture while lower strain rate resulted in solder-controlled fracture.[12] Besides, a shear test is an efficient way for evaluating the

(Received May 8, 2019; accepted July 24, 2019; published online August 5, 2019)

mechanical reliability of solder joints, since it is handy and less time-consuming. The shear test was also employed on aged samples to assess the impact of thermal aging on reliability of solder joints containing different levels of Ni addition.

In this study, Ni-doped solders are chosen and nickel effects on solders are thus focused on by setting up six specially designed sample conditions, Sn-1.2Ag-0.5Cu/OSP Cu, Sn-1.2Ag-0.5Cu-0.05Ni/OSP Cu and Sn-1.2Ag-0.5Cu-0.1Ni/OSP Cu, with the ball height of 300 μm before and after aging. The samples undergo a slow speed shear test in order to correlate the microstructures of solder balls with shear performance of solder joints.

MATERIALS AND METHODS

Sample Preparation

Commercial solder balls Sn-1.2Ag-0.5Cu-xNi (wt.%; SAC1205-xNi, x = 0, 0.05, 0.1) with the diameter of 300 μm were provided by Shenmao company. Solder balls were reflowed with the organic solderability preservative (OSP) Cu pad with 250-μm opening diameter on the printed circuit board (PCB). The reflow process was accomplished at peak temperature of 250°C for 40 s above the liquid temperature to produce attached specimens. In order to observe the microstructure and grain orientations with a scanning electron microscope (SEM) and electron back scattering diffraction (EBSD), the specimens were mechanically polished with 0.05 μm Al_2O_3 particles and etched with a rapid etching system.

Shear Testing

The shear tests were carried out using a multiple tester (Xyztec Sigma) with a fixed low shear speed, 250 μm/s. Lower shear speed guaranteed that the solders dominated the mechanical performance

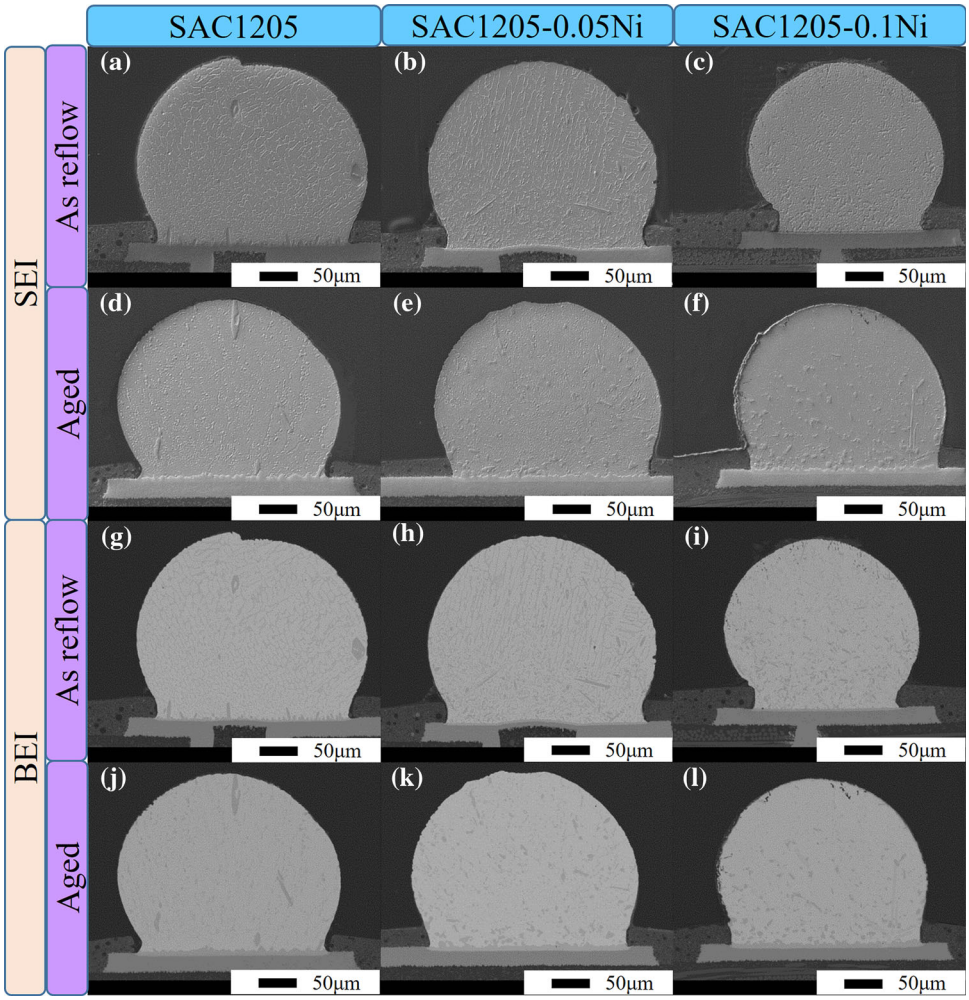

Fig. 1. Secondary electron images of (a) SAC1205/OSP Cu solder joints; (b) SAC1205-0.05Ni/OSP solder joints; (c) SAC1205-0.1Ni/OSP Cu solder joints; (d) Aged SAC1205/OSP Cu solder joints; (e) Aged SAC1205-0.05Ni/OSP solder joints; (f) Aged SAC1205-0.1Ni/OSP Cu solder joints; Back scattering electron images of (g) SAC1205/OSP Cu solder joints; (h) SAC1205-0.05Ni/OSP solder joints; (i) SAC1205-0.1Ni/OSP Cu solder joints; (j) Aged SAC1205/OSP Cu solder joints; (k) Aged SAC1205-0.05Ni/OSP solder joints; (l) Aged SAC1205-0.1Ni/OSP Cu solder joints.

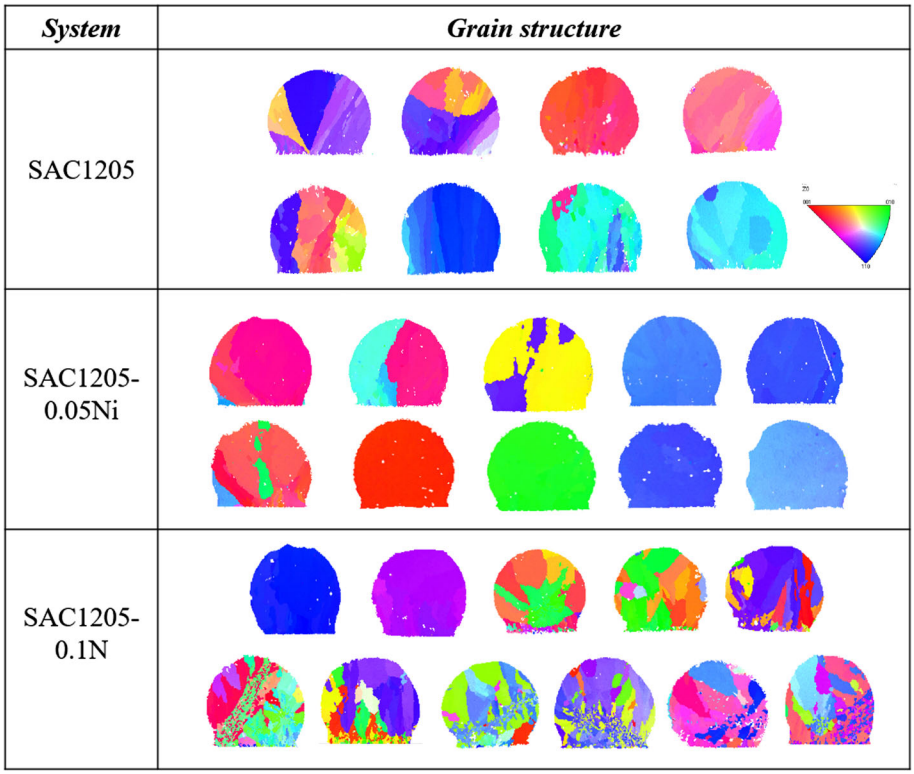

Fig. 2. EBSD orientation maps of SAC1205/OSP Cu, SAC1205-0.05Ni/OSP, and SAC1205-0.1Ni/OSP Cu solder joints.

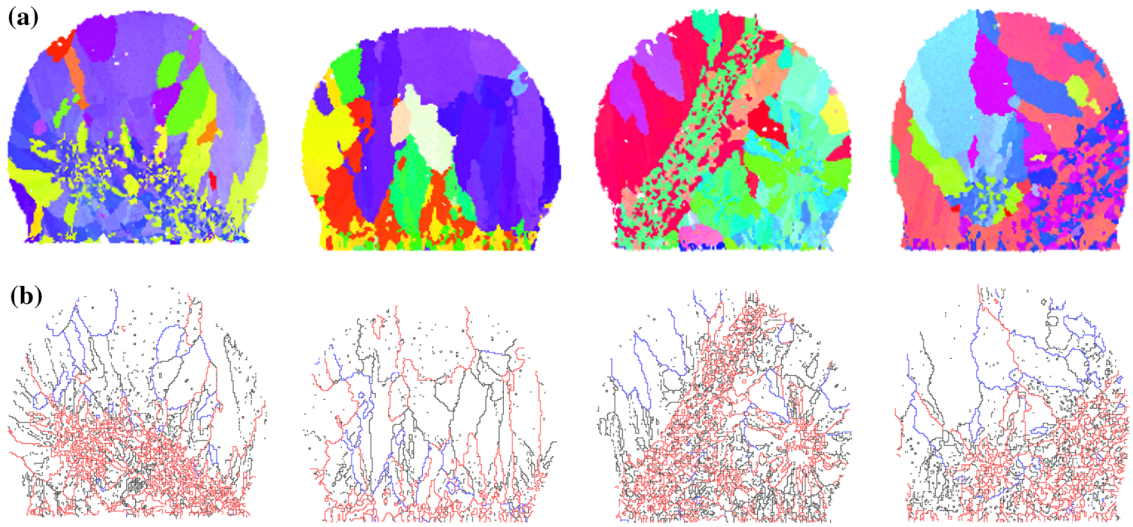

Fig. 3. (a) EBSD orientation maps of four chosen SAC1205-0.1Ni/OSP Cu solder joints. (b) Grain boundaries angle misorientation maps of corresponding SAC1205-0.1Ni/OSP solder joints.

rather than the interfacial IMCs. For all six systems, SAC1205-xNi (wt.%)/OSP Cu (x = 0, 0.05, 0.1) solder joints before and after aging, 300 samples in total were examined to attain statistical results.

Differential Scanning Calorimetry

For each system, 8–10 solder balls were reflowed on OSP Cu substrate, and then placed in an Al_2O_3 crucible for a differential scanning calorimetry (DSC) test. Samples were first heated to 250°C at the heating rate of 5°C/min. After reaching the peak temperature, the samples were cooled at the rate of 5°C/min to observe the solidification of each solder joint. Nitrogen gas flow of 20 mL/min was applied for the whole process to avoid oxidation. Undercooling was then defined by subtracting the onset

System	*Grain structure*
Aged SAC1205	
Aged SAC1205-0.05Ni	
Aged SAC1205-0.1N	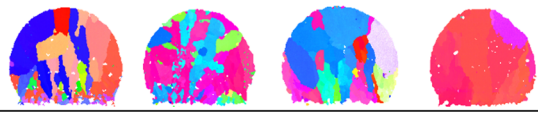

Fig. 4. EBSD orientation maps of aged SAC1205/OSP Cu, SAC1205-0.05Ni/OSP, and SAC1205-0.1Ni/OSP Cu solder joints.

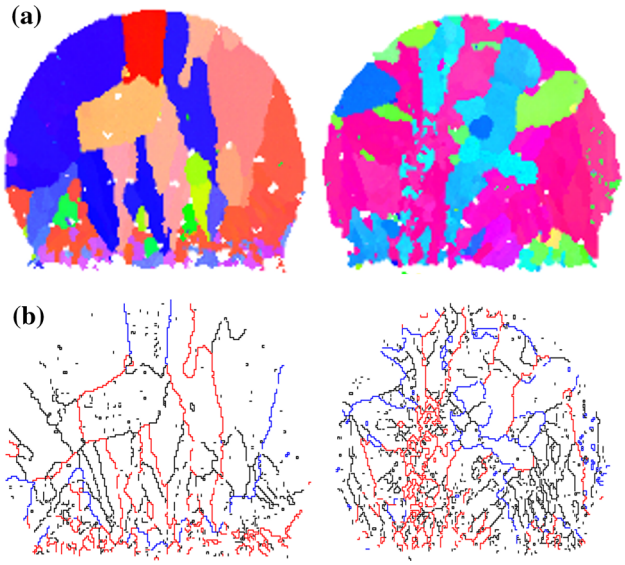

Fig. 5. (a) EBSD orientation maps of 2 chosen aged SAC1205-0.1Ni/OSP Cu solder joints. (b) Grain boundaries angle misorientation maps of corresponding aged SAC1205-0.1Ni/OSP solder joints.

temperature during melting by the averaged peak temperature during solidification.

RESULTS AND DISCUSSION

Figure 1 reveals the microstructure of as-reflow and aged SAC1205-xNi (wt.%)/OSP Cu (x = 0, 0.05, 0.1) solder joints. For as-reflow samples, massive IMCs precipitates and smoother interfacial IMCs were found after adding Ni into solders. Besides, the eutectic structure somewhat vanished when Ni content reached 0.1 wt.%. After aging the samples for 1000 h at 150°C, the IMCs in original eutectic structure of SAC1205/OSP Cu solder joints grew larger and thus caused the structure to fade away. Additionally, the eutectic structure nearly disappeared in the samples containing Ni. The IMCs precipitated and interfacial IMCs coarsened after isothermal aging.

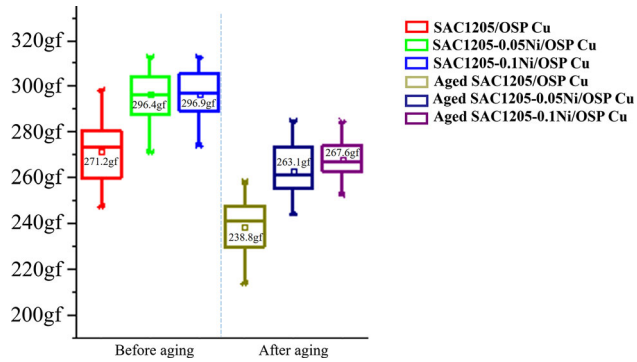

Fig. 6. Peak force in shear test of SAC1205-xNi (x = 0, 0.05, 0.1)/OSP Cu solder joints before and after aging.

Aside from microstructure, grain structure of as-reflowed samples observed with EBSD is shown below. Figure 2 reveals the orientation maps of as reflowed SAC1205/OSP Cu, SAC1205-0.05Ni/OSP Cu and SAC1205-0.1Ni/OSP Cu solder joints. SAC1205/OSP Cu and SAC1205-0.05Ni/OSP Cu solder balls showed relatively simple grain like single grain or beach-ball like grain. However, grain orientations of SAC1205-0.1Ni/OSP Cu were way more complicated. Two out of 11 examined samples were found to be single grain, three out of 11 were multiple grains, while rest of the six were multiple grains with partial area of fined grains. To evaluate the angles between adjacent grains in the fine grain zones, grain boundary angle misorientation mapping was conducted as shown in Fig. 3.

Figure 3 shows grain orientation maps and corresponding grain boundaries angle misorientation maps of four chosen SAC1205-0.1Ni/OSP Cu samples. In the boundaries angle misorientation maps, there are lines in three different colors: red, blue, and black, which represent grain boundary angles between 55° and 65°, grain boundary angle larger than 65° and grain boundary angle lower than 55°, respectively. By comparing Fig. 3a and b, the grain boundary angle misorientations of the fine grain

Table I. Undercooling of SAC1205-xNi/OSP Cu solder joints

DSC measurement temperature (Celsius)	Onset of melting	Average of solidification	Undercooling
SAC1205/OSP Cu	215.8	201.7	14.1
SAC1205-0.05Ni/OSP Cu	215.8	201.3	14.5
SAC1205-0.1Ni/OSP Cu	215.8	186.7	29.1

Table II. Peak force in shear tests of SAC1205-xNi/OPS Cu solder joints

Peak force (gf)	Average	Deviation
SAC1205	271.2	13.0
SAC1205-0.05Ni	296.4	10.8
SAC1205-0.1Ni	296.9	10.4
Aged SAC1205	238.8	11.9
Aged SAC1205-0.05Ni	263.1	11.8
Aged SAC1205-0.1Ni	267.6	8.2

zones are around 60°. These fine grains are the so-called interlaced structure.[13,14]

After aging the samples, the grain orientation remained about the same for SAC1205/OSP Cu and SAC1205-0.05Ni/OSP Cu solder joints as shown in Fig. 4. Nevertheless, interlaced structure barely existed in SAC1205-0.1Ni as the grain coarsened during long time aging. The boundary angle misorientation maps in Fig. 5 also illustrated that only little region of interlaced structure was discovered.

To understand how Ni affected the solidification process of SAC1205-xNi/OSP Cu solder joints, DSC was utilized to define the undercooling as shown in Table I. The results indicated that a certain concentration of Ni, somewhere between 0.05 wt.% and 0.1 wt.%, played an important role for increasing undercooling in SAC1205-xNi/OSP Cu solder joints. Regarding correlations between undercooling and fine grains,[13] results in Table I matched well with the orientation maps in Fig. 2. SAC1205-0.05Ni/OSP Cu and SAC1205/OSP Cu solder joints exhibited similar undercooling and grain structure. However, SAC1205-0.1Ni/OSP Cu solder joints possessed nearly doubled undercooling of other systems and more complex grain structure.

Distinct microstructure of solder joints leads to different mechanical properties. With the aid of a slow speed shear test, correlations between the microstructure and shear performance can be examined. As shown in Fig. 6 and Table II, both SAC1205-0.05Ni/OSP Cu solder joints and SAC1205-0.1Ni/OSP Cu solder joints exhibit a 9% enhancement as compared to SAC1205/OSP Cu solder joints before aging. As for aged conditions, though the peak force degraded comprehensively, solder joints with Ni doping still showed better performance. Relatively, SAC1205-0.05Ni/OSP Cu solder joints were enhanced by 10% and SAC1205-0.1Ni/OSP Cu solder joints were enhanced by 12% as compared to solder joints without Ni. Minor doping of Ni brought significant benefit to mechanical reliability of SAC1205/OSP Cu solder joints.

The dominating factor of the increment in a shear test after adding Ni is the precipitations in solder balls. Ni serves as nucleation sites for IMCs, which reinforce the effect of precipitates strengthening. The spread tiny precipitates in Ni-doped solder balls hinder the propagation of dislocations and then enhance the mechanical reliability. Moreover, the finer grain and interlaced area are believed to complicate the path of dislocations propagation and thus improve the mechanical performance slightly.

CONCLUSIONS

In SAC 1205-xNi/OSP Cu solder joints, the microstructure is altered due to the existence of nickel. Ni serves as nucleation sites for IMCs, and in turn, Ni affects the undercooling of solder joints and thus triggers finer or interlaced grain structure. Shear tests were carried out to examine the mechanical reliability of solder joints, and slow velocity was chosen to focus on the changes in solder balls. The results showed that the mechanical performance of SAC1205-0.1Ni/OSP Cu and SAC1205-0.05Ni/OSP Cu solder joints were superior to that of SAC1205/OSP Cu solder joints regardless of before or after aging. The fine grains and the spread tiny precipitates are attributed to nickel doping, which brings benefits to mechanical performance. To sum up, doping a small amount of nickel into 300 μm low-silver solder balls alters microstructure and improves the mechanical reliability of BGA in electronics packaging.

ACKNOWLEDGMENTS

The financial support from the Ministry of Science and Technology, Taiwan, under the Contract No. MOST 107-2221-E-007-090 and technical support from Shenmao are much appreciated.

REFERENCES

1. K.N. Tu and K. Zeng, in *Electronic Components & Technology Conference Proceedings* (2002), pp. 1194–1200.
2. F.X. Che, W.H. Zhu, E.S.W. Poh, X.W. Zhang, and X.R. Zhang, *J. Alloys Compd.* 507, 215–224 (2010).
3. F. Cheng, F. Gao, J. Zhang, W. Jin, and X. Xiao, *J. Mater. Sci.* 46, 3424–3429 (2011).
4. P.L.A.F. Guo, in *Electronics Packaging Technology Conference Proceedings* (2006), pp. 717–721.

5. A.I.E., Development of Sn-Ag-Cu and Sn-Ag-Cu-X alloys for Pb-free electronic solder applications. In: Lead-Free Electronic Solders. (Springer, Boston, MA, 2006), pp. 55–76.
6. A.A. El-Daly, A.E. Hammad, A. Fawzy, and D.A. Nasrallh, *Mater. Des.* 43, 40 (2013).
7. P. Liu, P. Yao, and J. Liu, *J. Alloys Compd.* 486, 474 (2009).
8. C.-Y. Yu, T.-K. Lee, M. Tsai, K.-C. Liu, and J.-G. Duh, *J. Electron. Mater.* 39, 2544 (2010).
9. C. Fleshman, W.-Y. Chen, T.-T. Chou, J.-H. Huang, and J.-G. Duh, *Mater. Chem. Phys.* 189, 76 (2017).
10. R. Kinyanjui, L.P. Lehman, L. Zavalij, and E. Cotts, *J. Mater. Res.* 20, 2914 (2011).
11. B.S.S. Chandra Rao, J. Weng, L. Shen, T.K. Lee, and K.Y. Zeng, *Microelectron. Eng.* 87, 2416 (2010).
12. K.E. Yazzie, H.X. Xie, J.J. Williams, and N. Chawla, *Scripta Mater.* 66, 586 (2012).
13. B. Arfaei, N. Kim, and E.J. Cotts, *J. Electron. Mater.* 41, 362 (2011).
14. L.P. Lehman, Y. Xing, T.R. Bieler, and E.J. Cotts, *Acta Mater.* 58, 3546 (2010).